

Material/Geometry Adaptive Shape Functions for Rayleigh–Ritz Vibration Analysis of Composite Plates

Jong-Eun Kim* and Nesrin Sarigul-Klijn†
University of California, Davis, Davis California 95616

New shape functions, which are adapted to changes of aspect ratio and material properties of composite plates referred as material/geometry adaptive shape functions, have been developed to improve the accuracy of the Rayleigh–Ritz method for vibration analyses. The comparisons of free vibration analysis using these adaptive shape functions to the mode shapes from literature show suitability and accuracy of these adaptive shape functions. These shape functions and the frequency equations of composite plates are presented for five different cases of boundary conditions. To obtain accurate results, up to 13 modes are used in the Rayleigh–Ritz formulation. The effect of ply orientation angle on the vibration response using this method is investigated. The results of free vibration responses using new adaptive shape functions show excellent agreement with those of finite element analysis.

Introduction

THE Rayleigh–Ritz (R–R) method is a simple modal approximation approach for computing plate deflections and is widely used in many applications including aeroelastic instability prediction of lifting surfaces.^{1–3} Although the R–R method has limited applicability when applied to complex geometries, it still is attractive due to its capability to yield superior accuracy with minimal computational requirements. The accuracy of the R–R method is highly dependent on the shape functions assumed to represent the actual deformations. The assumed shape functions must at least satisfy the geometric boundary conditions. For example, for aeroelastic analysis of rectangular lifting surfaces simulated by a cantilevered plate, the shape functions of beam bending and torsion modes have been used for the predictions of the plate bending and torsion modes.

In this paper, a new shape function extraction method is presented to predict the vibration modes of composite plates accurately without increasing computational costs using five different cases of plate boundary conditions. Note that Hamilton's principle allows extraction of the shape functions for not only the bending modes but also the torsion modes. The suggested shape functions are adaptive to changes of aspect ratio and material properties such as the thickness, fiber orientation, and stacking sequence of the individual plies of composite plates.

R–R Formulation

Hamilton's principle for a nonconservative elastic system is expressed as

$$\delta \int_{t_1}^{t_2} (T - V) dt + \int_{t_1}^{t_2} \delta W dt = 0 \quad (1)$$

where δW is the virtual work done by external forces and t_1 and t_2 are the initial and final times of the motion, respectively. The kinetic energy for a plate neglecting in-plane displacements is given by

$$T = \frac{1}{2} \int_0^L \int_{-c/2}^{c/2} \left(\frac{dw}{dt} \right)^2 \rho dy dx \quad (2)$$

where ρ is the mass per unit area and w is the transverse deflection. The strain energy for a symmetric anisotropic laminated plate (Fig. 1) neglecting in-plane displacements is given as⁴

$$V = \frac{1}{2} \int_0^L \int_{-c/2}^{c/2} \left[D_{11} \left(\frac{\partial^2 w}{\partial x^2} \right)^2 + 2D_{12} \frac{\partial^2 w}{\partial x^2} \frac{\partial^2 w}{\partial y^2} + D_{22} \left(\frac{\partial^2 w}{\partial y^2} \right)^2 + 4D_{16} \frac{\partial^2 w}{\partial x^2} \frac{\partial^2 w}{\partial x \partial y} + 4D_{26} \frac{\partial^2 w}{\partial y^2} \frac{\partial^2 w}{\partial x \partial y} + 4D_{66} \left(\frac{\partial^2 w}{\partial x \partial y} \right)^2 \right] dy dx \quad (3)$$

where D_{ij} are the flexural moduli, which depend on the fiber orientation and stacking sequence of the individual laminas. The R–R method begins with assuming structural deformation shapes by superposition of a finite number of shape functions given as

$$w = \sum_{i=1}^n \gamma_i(x, y) q_i(t) \quad (4)$$

where $q_i(t)$ is the generalized displacement of the i th mode, n is the total number of modes, and $\gamma_i(x, y)$ are the approximate deformations or shape functions. These are

$$\gamma_i(x, y) = \Phi_i(x) \Psi_i(y) \quad (5)$$

where $\Phi(x)$ and $\Psi(y)$ are independent shape functions of x and y , respectively. When Eq. (5) is substituted into Eqs. (2–4) and Lagrange's equation, the system matrix for free vibration can be expressed in a matrix form as

$$[M] \ddot{q}_i + [K] q_i = 0 \quad (6)$$

where $[M]$ and $[K]$ are $n \times n$ mass and stiffness matrices, respectively.

New Shape Functions for Torsion and y-Direction Bending Modes

The accuracy of the R–R method is highly dependent on the shape functions chosen to represent the deformation shapes of a plate. In the case that the plate has two opposite free edges parallel to the x direction and the other two edges parallel to the y direction as either built-in (clamped), simple supported or free, the x -direction bending, torsion, and y -direction bending modes can represent three types of primary deformation shapes for moderate ranges of aspect ratio. The aspect ratio \mathcal{R} of the plate is defined as a ratio of the x -direction length L to the y -direction length c ($\mathcal{R} = L/c$). The chosen shape functions must satisfy geometric boundary conditions

Received 1 March 2000; revision received 17 August 2000; accepted for publication 1 September 2000. Copyright © 2000 by the American Institute of Aeronautics and Astronautics, Inc. All rights reserved.

*Graduate Research Assistant, Department of Mechanical and Aeronautical Engineering, Student Member AIAA.

†Professor, Department of Mechanical and Aeronautical Engineering, Senior Member AIAA.

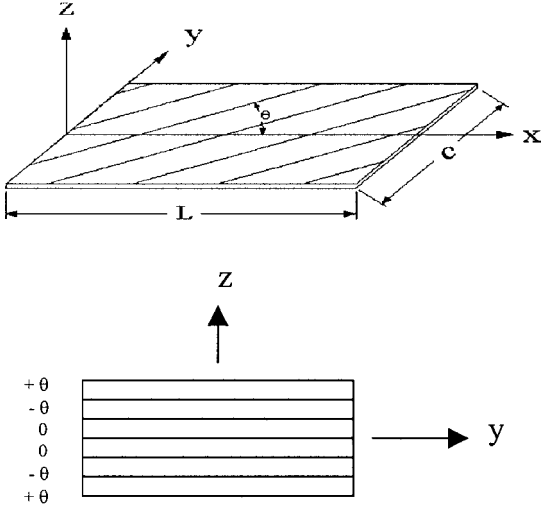


Fig. 1 Composite plate model layout ($[\pm \theta/0]_s$ laminate).

at a minimum. The beam torsion mode (based on St. Venant's theory) has been used for the torsion mode of cantilevered plates^{1,2,5}

$$\Phi_{Tm}(x) = \sin(m\pi x/2L), \quad \Psi_T(y) = y/c$$

$$m = 1, 3, 5, 7, \dots \quad (7)$$

Note that $\Phi_{Tm}(x)$ in Eq. (7) does not satisfy the geometric boundary condition of a cantilevered plate ($d\Phi/dx \neq 0$ at $x=0$). Moreover, in the same references the assumption that the midspan has maximum y-direction curvature for y-direction bending mode

$$\Phi_C(x) = (x/L)(1 - x/L), \quad \Psi_C(y) = 4(y/c)^2 - \frac{1}{3} \quad (8)$$

results in $\Phi_C(x)$ that does not satisfy the geometric boundary condition. In the next section, new x-direction shape functions Φ_T and Φ_C that satisfy all of the boundary conditions of a plate will be suggested.

New Shape Function Extraction Method

To formulate shape functions to represent accurately the deformed shape, the following procedure is suggested. When Eq. (5) is substituted into Eqs. (2-4), variation on Eq. (1) is taken, and simple harmonic motion is assumed, one governing equation for x-direction shape function Φ is obtained:

$$\frac{d^4\Phi}{d\tilde{x}^4} + \left[\frac{2a_2L^2}{a_1} \frac{D_{12}}{D_{11}} - \frac{4a_4L^2}{a_1} \frac{D_{66}}{D_{11}} \right] \frac{d^2\Phi}{d\tilde{x}^2} + \left[\frac{a_3L^4}{a_1} \frac{D_{22}}{D_{11}} - \omega^2 \frac{\rho L^4}{D_{11}} \right] \Phi = 0 \quad (9)$$

where \tilde{x} is the nondimensional coordinate $\tilde{x} = x/L$ and the boundary equations are

$$\left. \frac{d(\delta\Phi)}{d\tilde{x}} \right|_0^1 \left\{ D_{11}a_1 \frac{d^2\Phi}{d\tilde{x}^2} + 2D_{16}a_5L \frac{d\Phi}{d\tilde{x}} + D_{12}a_2L^2\Phi \right\} = 0$$

$$\delta\Phi|_0^1 \left\{ -D_{11}a_1 \frac{d^3\Phi}{d\tilde{x}^3} + (4D_{66}a_4 - D_{12}a_2)L^2 \frac{d\Phi}{d\tilde{x}} + 2D_{26}a_6L^3\Phi \right\} = 0 \quad (10)$$

The unknown coefficients are

$$a_1 = \int_{-c/2}^{c/2} \Psi^2 dy, \quad a_2 = \int_{-c/2}^{c/2} \Psi \frac{d^2\Psi}{dy^2} dy$$

$$a_3 = \int_{-c/2}^{c/2} \left(\frac{d^2\Psi}{dy^2} \right)^2 dy, \quad a_4 = \int_{-c/2}^{c/2} \left(\frac{d\Psi}{dy} \right)^2 dy$$

$$a_5 = \int_{-c/2}^{c/2} \Psi \frac{d\Psi}{dy} dy, \quad a_6 = \int_{-c/2}^{c/2} \frac{d\Psi}{dy} \frac{d^2\Psi}{dy^2} dy \quad (11)$$

If $\Psi(y)$ is given, Eq. (9) becomes an ordinary differential equation as a function of Φ only. For each mode $\Psi(y)$ can be assumed as follows.^{1,2,5}

For pure x-direction bending mode:

$$\Psi(y) = 1 \quad (12a)$$

For pure torsion mode:

$$\Psi(y) = y/c \quad (12b)$$

For pure y-direction bending mode:

$$\Psi(y) = 4(y/c)^2 - \frac{1}{3} \quad (12c)$$

In the case of a pure x-direction bending mode, the coefficients become

$$a_1 = c, \quad a_2 = a_3 = a_4 = a_5 = a_6 = 0 \quad (13)$$

Therefore, the governing equation becomes

$$\frac{d^4\Phi}{d\tilde{x}^4} - \beta^4\Phi = 0 \quad (14)$$

where

$$\beta^4 = \omega^2 \rho L^4 / D_{11}$$

This equation yields the same shape functions and frequency equations as the transverse vibration of a beam.⁶

In the case of a pure torsion mode along the x direction, the coefficients become

$$a_1 = c/12, \quad a_4 = 1/c, \quad a_2 = a_3 = a_5 = a_6 = 0 \quad (15)$$

Therefore, the governing equation becomes

$$\beta_T \frac{d^4\Phi}{d\tilde{x}^4} - \frac{d^2\Phi}{d\tilde{x}^2} - k_T^2\Phi = 0 \quad (16)$$

where

$$\beta_T = \frac{D_{11}}{48D_{66}\mathcal{R}^2}, \quad k_T^2 = \frac{\omega^2 \rho L^4}{48D_{66}\mathcal{R}^2}$$

The solution of $\Phi(\tilde{x})$ can be obtained by letting $k_T^2 = g_T^2(1 + \beta_T g_T^2)$ as follows:

$$\Phi(\tilde{x}) = B_1 \cos g_T \tilde{x} + B_2 \sin g_T \tilde{x} + B_3 \cosh f_T \tilde{x} + B_4 \sinh f_T \tilde{x} \quad (17)$$

where $f_T^2 = g_T^2 + 1/\beta_T$.

In the case of a pure y-direction bending mode, the coefficients become

$$a_1 = 4c/45, \quad a_3 = 64/c^3, \quad a_4 = 16/3c$$

$$a_2 = a_5 = a_6 = 0 \quad (18)$$

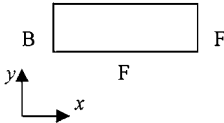
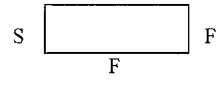
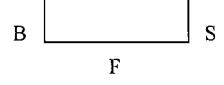
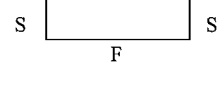
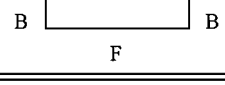
Therefore, the governing equation becomes

$$\beta_C \frac{d^4\Phi}{d\tilde{x}^4} - \frac{d^2\Phi}{d\tilde{x}^2} - k_C^2\Phi = 0 \quad (19)$$

where

$$\beta_C = \frac{D_{11}}{240D_{66}\mathcal{R}^2}, \quad k_C^2 = \frac{\omega^2 \rho c^2 L^2}{240D_{66}} - 3\mathcal{R}^2 \frac{D_{22}}{D_{66}}$$

Table 1 Composite plate x -direction shape functions and frequency equations for pure torsion modes

Cases	Boundary conditions	x -Direction shape functions [frequency equations]
B-F		$\Phi_{Ti}(\tilde{x}) = \sin g_{Ti} \tilde{x} + (g_{Ti}/f_{Ti})(\cosh f_{Ti} \tilde{x} - \sinh f_{Ti} \tilde{x} - \cos g_{Ti} \tilde{x})$ $2g_{Ti}^2 f_{Ti}^2 + (g_{Ti} f_{Ti}^4 - g_{Ti}^3 f_{Ti}^2) \sin g_{Ti} \sinh f_{Ti} + (f_{Ti}^5 + g_{Ti}^4 f_{Ti}) \cos g_{Ti} \cosh f_{Ti} = 0$
S-F		$\Phi_{Ti}(\tilde{x}) = \sin g_{Ti} \tilde{x} + \frac{g_{Ti}^2 \sin g_{Ti}}{f_{Ti}^2 \sinh f_{Ti}} \sinh f_{Ti} \tilde{x}$ $g_{Ti}^3 \sin g_{Ti} \cosh f_{Ti} - f_{Ti}^3 \cos g_{Ti} \sinh f_{Ti} = 0$
B-S		$\Phi_{Ti}(\tilde{x}) = \sin g_{Ti} \tilde{x} + \frac{g_{Ti}}{f_{Ti}} (\cosh f_{Ti} \tilde{x} - \sinh f_{Ti} \tilde{x} - \cos g_{Ti} \tilde{x})$ $(g_{Ti}^2 f_{Ti} + f_{Ti}^3) \sin g_{Ti} \cosh f_{Ti} - (g_{Ti}^3 + g_{Ti} f_{Ti}^2) \cos g_{Ti} \sinh f_{Ti} = 0$
S-S		$\Phi_{Ti}(\tilde{x}) = \sin g_{Ti} \tilde{x} - \frac{\sin g_{Ti}}{\sinh f_{Ti}} \sinh f_{Ti} \tilde{x}, \quad (g_{Ti}^2 + f_{Ti}^2) \sin g_{Ti} \sinh f_{Ti} = 0$
B-B		$\Phi_{Ti}(\tilde{x}) = \sin g_{Ti} \tilde{x} + \frac{g_{Ti}}{f_{Ti}} (\cosh f_{Ti} \tilde{x} - \sinh f_{Ti} \tilde{x} - \cos g_{Ti} \tilde{x})$ $2g_{Ti} f_{Ti} + (f_{Ti}^2 - g_{Ti}^2) \sin g_{Ti} \sinh f_{Ti} - 2g_{Ti} f_{Ti} \cos g_{Ti} \cosh f_{Ti} = 0$

The solution of $\Phi(\tilde{x})$ can be obtained by letting $k_c^2 = g_c^2(1 + \beta_c g_c^2)$ as follows:

$$\Phi(\tilde{x}) = B_1 \cos g_c \tilde{x} + B_2 \sin g_c \tilde{x} + B_3 \cosh f_c \tilde{x} + B_4 \sinh f_c \tilde{x} \tag{20}$$

where $f_c^2 = g_c^2 + 1/\beta_c$.

Adaptive Shape Functions for Five Distinct Cases

In this section, the x -direction shape functions and frequency equations for torsion and y -direction bending modes of a composite plate are formulated for five distinct cases of different boundary conditions.⁷ For each case, four independent linear homogeneous equations, which are obtained by substituting two edge conditions into Eq. (17), result in the x -direction shape function and frequency equation for torsion mode, which are given in Table 1. The edge conditions for torsion modes are obtained from Eq. (10).

For built-in edge (B)

$$\Phi = 0, \quad \frac{d\Phi}{d\tilde{x}} = 0 \tag{21a}$$

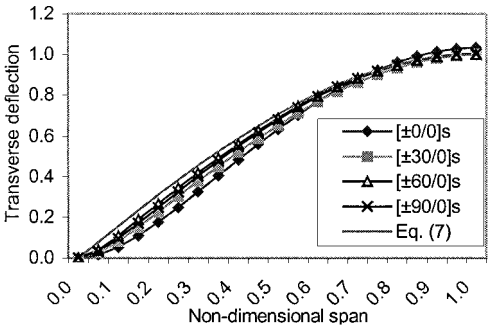
For simple support edge (S)

$$\Phi = 0, \quad \frac{d^2\Phi}{d\tilde{x}^2} = 0 \tag{21b}$$

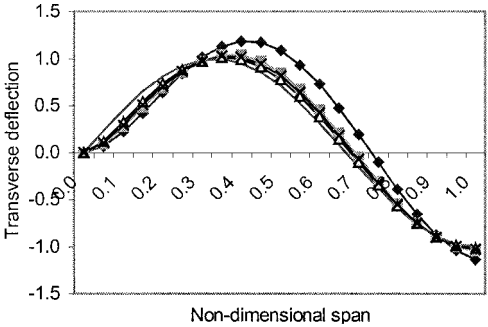
For free edge (F)

$$\frac{d^2\Phi}{d\tilde{x}^2} = 0, \quad \beta_T \frac{d^3\Phi}{d\tilde{x}^3} - \frac{d\Phi}{d\tilde{x}} = 0 \tag{21c}$$

The shape function for the built-in-free (B-F) case in Table 1 is identical to the results of the partial Ritz analysis (see Refs. 8 and 9), which assumes $\gamma(x, y)$ as $[\tilde{\gamma}(x) + y\theta(x)]$, where $\tilde{\gamma}(x)$ and $\theta(x)$ are independent functions of x . Through this partial Ritz analysis, however, the shape function for y -direction bending mode cannot be obtained because the y -direction vibration mode is excluded. In the procedure presented herein, the shape functions for the y -direction bending mode can be easily obtained by applying the similar step to find the torsion mode. The x -direction shape functions and frequency equations for y -direction bending modes are identical to



a) First mode



b) Second mode

Fig. 2 Comparisons of x -direction shape functions for torsion mode, $\mathcal{AR} = 4$, B-F case.

torsion modes with the exception that β_c , g_c , and f_c are substituted for β_T , g_T , and f_T , respectively.

The proposed shape functions are adaptive to changes of \mathcal{AR} and material properties such as the ply thickness, fiber orientation angle, and stacking sequence. The adaptability is a result of choosing the shape functions based on the coefficients g_{Ti} and f_{Ti} , which are calculated from frequency equations (see Table 1). The f_{Ti} is function of β_T , which includes \mathcal{AR} and flexibility modulus D_{ij} . Figure 2

shows the x -direction shape functions for the torsion mode to show the adaptability of new shape functions to changes of ply orientation angle and the comparison with beam torsion mode in Eq. (7). Figure 3 shows the assumed y -direction bending mode using the new adaptive shape functions as compared to one from the literature [Eq. (8)] demonstrating the suitability of the proposed functions. Unlike the mode obtained using Eq. (8) based on the assumption that the midspan has maximum y -direction curvature, the new shape functions yield a mode that shows the maximum y -direction curvature to appear at the plate tip for the B-F case. In addition, these functions satisfy all of the geometric boundary conditions.

The suggested shape functions are for pure bending and pure torsion modes, which means that coupled mode shapes and stiffness coupling terms D_{12} , D_{16} , and D_{26} are not considered in these shape functions. To take into account the coupling effects of these modes in the analysis, up to six x -direction bending (B) modes, up to six torsion (T) modes, and one y -direction bending (C) mode are used in the R-R formulation. The bending-torsion coupling effects are included during constitution of the stiffness K matrix as off-diagonal terms.

Results and Discussion

The material properties of Hercules AS1/3501-6 graphite/epoxy are used in this effort. To compare the results of the R-R method, a finite element analysis (FEA) using 400 thin plate elements is conducted. A commercial code ABAQUS, version 5.6, was available for this purpose.

In this work the total number of modes for the R-R formulation is extended up to 13 modes to obtain accurate results. The 13, 11, 9, and 7 modes in Table 2 indicate the total number of modes consisting of 6B + 6T + 1C, 5B + 5T + 1C, 4B + 4T + 1C, and 3B + 3T + 1C, respectively. As it can be seen from the numerical results, the anal-

ysis using a large number of modes shows better agreement with results using FEA.

Table 3 shows the results of free vibration analysis using the new shape functions compared to the results using the functions in Eqs. (7) and (8). The results show that the analysis using the new functions yields improved solutions, and the first y -direction bending mode of FEA is identical to the assumed shape using the new shape functions, as shown in Fig. 3b.

Figure 4 shows the effects of ply orientation angle on the free vibration response using the new shape functions. The $[\pm 45/0]_s$ laminate has the highest natural frequency for torsion modes, and the $[\pm 0/0]_s$ laminate has the highest natural frequency for x -direction bending modes, due to the stiffness directionalities of the composite plates.

Finally, Table 4 shows the results from the free vibration analyses of composite plates with various boundary conditions consisting of B-F, S-F, B-S, S-S, and B-B. The results of the R-R method using the new functions show excellent agreement with FEA results.

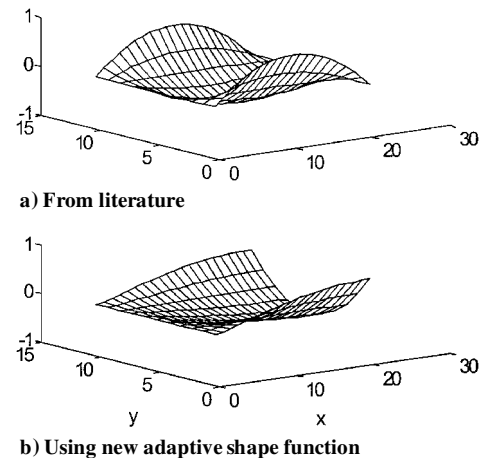


Fig. 3 Assumed pure y -direction bending mode of a plate for B-F case.

Table 2 Convergence test of natural frequencies (Hz) using new shape functions, $\mathcal{R} = 2$ ($L = 0.1524$), B-F case, $[\pm 45/0]_s$ laminate

Mode ^a	FEA	Modes			
		13	11	9	7
1B	24.09	25.03	25.21	25.22	25.25
1T	141.51	140.72	144.36	144.44	144.45
2B	151.36	153.82	154.76	156.98	157.04
2T	458.17	490.98	494.36	495.15	497.44
1C	702.02	782.77	785.86	825.63	865.54

^aFirst (1) and second (2) modes respectively.

Table 3 Comparison of natural frequencies (Hz), $\mathcal{R} = 1$ ($L = 0.0762$), B-F case, $[\pm 45/0]_s$ laminate

Mode	FEA	New shape functions	Shape functions from literature
1B	100.76	102.97 (2.19) ^a	99.64 (1.12)
1T	320.92	334.33 (4.18)	284.11 (11.47)
2B	600.20	604.28 (0.68)	632.94 (5.48)
1C	859.14	977.16 (13.74)	1032.95 (20.23)
2T	1098.40	1173.36 (6.82)	1495.14 (36.12)

^a(% Error = |FEA - R-R method|/FEA \times 100.)

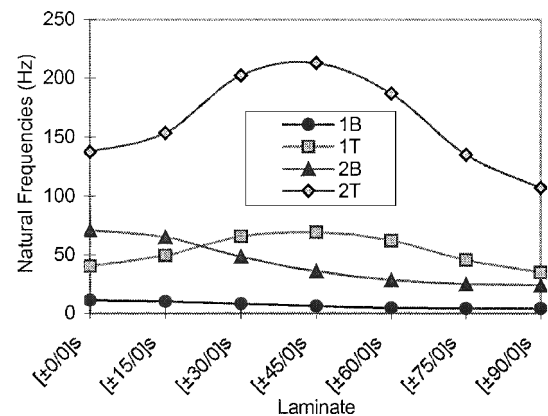


Fig. 4 Effects of ply orientation angle on the free vibration response, $\mathcal{R} = 4$, B-F case.

Table 4 Natural frequencies (Hz) for various cases of boundary conditions, $\mathcal{R} = 4$, $[\pm 30/0]_s$ laminate

Mode	B-F	S-F ^a	B-S	S-S	B-B
1	8.2 (7.9) ^b	32.8 (32.6)	34.6 (35.1)	21.6 (21.9)	50.2 (52.4)
2	47.9 (48.9)	61.5 (61.2)	107.5 (111.4)	85.3 (85.8)	132.2 (136.4)
3	65.6 (65.2)	111.4 (110.2)	140.3 (136.1)	128.0 (127.0)	157.5 (150.1)
4	135.6 (139.3)	191.4 (188.3)	226.7 (237.0)	198.0 (199.1)	269.4 (276.4)
5	202.8 (200.8)	222.5 (234.9)	298.9 (285.4)	283.2 (266.6)	327.4 (308.2)
6	265.9 (276.0)	340.3 (331.8)	431.9 (404.2)	337.2 (356.2)	448.5 (452.5)
7	380.9 (353.2)	410.7 (402.4)	458.4 (468.2)	407.4 (435.8)	503.8 (506.9)

^aSkip rigid-body mode. ^b(FEA results.)

Conclusions

New shape functions have been developed to improve the accuracy of the R-R method and are herein applied to free vibration analyses of composite plates with different boundary conditions. Unlike other studies, the suggested shape functions are adaptive to changes of aspect ratio and material properties of composite plates and satisfy all of the geometric boundary conditions. The plots of assumed mode shapes using new adaptive shape functions, together with the results of free vibration analyses, show the suitability and accuracy of the proposed functions. The shape functions and frequency equations for five different cases of boundary conditions are presented. The effects of ply orientation angle on the vibration response are also provided. The results of the R-R method using the new adaptive shape functions show excellent agreement with those of finite element analyses.

References

- ¹Hollowell, S. J., and Dugundji, J., "Aeroelastic Flutter and Divergence of Stiffness Coupled, Graphite/Epoxy, Cantilevered Plates," *Journal of Aircraft*, Vol. 21, No. 1, 1984, pp. 69–76.
- ²Landsberger, B. J., and Dugundji, J., "Experimental Aeroelastic Behavior of Unswept and Forward-Swept Cantilever Graphite/Epoxy Wings" *Journal of Aircraft*, Vol. 22, No. 8, 1985, pp. 679–686.
- ³Sarigul-Klijn, N., and Oguz, S., "Effect of Aspect Ratio and Ply Orientation on Aeroelastic Response of Composite Plates," *Journal of Aircraft*, Vol. 35, No. 4, 1998, pp. 657–659.
- ⁴Whitney, J. M., *Structural Analysis of Laminated Anisotropic Plates*, Technomic, Lancaster, PA, 1987, pp. 41–44.
- ⁵Jensen, D. W., and Crawley, E. F., "Frequency Determination Techniques for Cantilevered Plates with Bending-Torsion Coupling," *AIAA Journal*, Vol. 22, No. 3, 1984, pp. 415–420.
- ⁶Rao, S. S., *Mechanical Vibrations*, 3rd ed., Addison-Wesley, Reading, MA, 1995, pp. 523–541.
- ⁷Kim, J. E., "An Approach to Elastic-Dynamic-Aeroelastic Multiobjective Optimization of Rotor Blades," Ph.D. Dissertation, Mechanical and Aeronautical Engineering Dept., Univ. of California, Davis, CA, 2000, pp. 49–69.
- ⁸Crawley, E. F., and Dugundji, J., "Frequency Determination and Non-Dimensionalization for Composite Cantilever Plates," *Journal of Sound and Vibration*, Vol. 72, No. 1, 1980, pp. 1–10.
- ⁹Jensen, D. W., Crawley, E. F., and Dugundji, J., "Vibration of Cantilevered Graphite/Epoxy Plates with Bending-Torsion Coupling," *Journal of Reinforced Plastics and Composites*, Vol. 1, No. 2, 1982, pp. 254–269.